

Article

Physicochemical, Performance, Combustion and Emission Characteristics of Melaleuca Cajuputi Oil-Refined Palm Oil Hybrid Biofuel Blend

Sharzali Che Mat ^{1,2} , Mohamad Yusof Idroas ^{1,*}, Yew Heng Teoh ¹ and Mohd Fadzli Hamid ¹

¹ School of Mechanical Engineering, Engineering Campus, Universiti Sains Malaysia, Nibong Tebal 14300, Malaysia; sharzali.chemat@ppinang.uitm.edu.my (S.C.M.); yewhengteoh@usm.my (Y.H.T.); mohd_fadzli@outlook.com (M.F.H.)

² Faculty of Mechanical Engineering, Universiti Teknologi MARA Pulau Pinang, Permatang Pauh 13500, Malaysia

* Correspondence: meyusof@usm.my; Tel.: +604-5996-301

Received: 13 September 2018; Accepted: 28 September 2018; Published: 14 November 2018



Abstract: To reduce the economic impact caused by the fossil fuel crisis and avoid relying on existing biofuels, it is important to seek locally available and renewable biofuel throughout the year. In the present work, a new light biofuel—Melaleuca Cajuputi oil (MCO)—was introduced to blend with refined palm oil (RPO). The physicochemical properties, combustion characteristics, engine performance, and exhaust emissions were comprehensively examined. It was found that the higher the percentage of MCO, the lower the viscosity and density of the blends obtained. Calorific value (CV) was increased with the increase of MCO fraction in the blend. Regression analysis has suggested that the blend of 32% (*v/v*) of RPO and 68% (*v/v*) of MCO (RPO32MCO68) is optimal to obtain viscosity and density in accordance with ASTM 6751/EN 14214 standards. The experimental results show that the in-cylinder pressure, brake torque, and brake power of the optimal blend were slightly lower than those of baseline diesel fuel. Brake specific fuel consumption (BSFC), carbon monoxide (CO), and unburnt hydrocarbon (HC) were found to be slightly higher compared to diesel fuel. Notably, nitrogen oxides (NO_x) and smoke opacity were found to be decreased over the entire range of the test. Overall, the optimal blend of RPO32MCO68 has shown a decent result which marks it as a potential viable source of biofuel.

Keywords: Melaleuca Cajuputi oil; refined palm oil; hybrid biofuel; viscosity; binary blend

1. Introduction

The rising demand for global energy, depletion of fossil fuel, and concern over environmental issues has led to an intensive search for renewable and reliable biofuel. The fluctuation of crude oil price and currency exchange rate could affect the energy supply and economics of those countries that solely depend on imported oil from others. To reduce the economic impact caused by the fuel crisis, it is important to seek biofuel which is available locally and renewable throughout the year. Thus, continuous effort in the search for new energy resources is very important to ensure energy security for the future.

Over the past decades, straight vegetable oils (SVOs) have gained interest among researchers as a potential fossil fuel replacement. Their comparable properties to diesel, nontoxicity, and the absence of sulfur content make them an attractive alternative biofuel. At present, the European Union is the major producer of rapeseed and sunflower oils, while soybean, palm, and coconut oils are largely produced in the United States, South East Asia, and Philippines, respectively [1]. At present, over 95% of biodiesel produced globally is from edible vegetable oil [2].

Typical edible SVOs, such as sunflower, soybean, rapeseed, and palm oils, have been extensively studied and short-term tests revealed that those SVOs can be used directly on a compression ignition (CI) engine [3–7]. Notably, SVOs have slightly lower engine performance compared to diesel fuel. In general, nitrogen oxide (NO_x) emission was lower whereby carbon monoxide (CO) and hydrocarbon (HC) emissions were higher than diesel fuel. Nonetheless, the brake specific fuel consumption (BSFC) of all tested fuels is higher than diesel fuel. Higher BSFC is associated with high viscosity and low calorific value of the vegetable oil [8,9].

However, due to the concern over competition between food supply and fuel, extensive studies on non-edible vegetable oil have been carried out for the past decade. Jatropha, mahua, linseed, rubber, karanja, and cottonseed oil are among the non-edible oils that receive attention from many researchers [10–14]. Various blends of non-edible oil with diesel or biodiesel were found to have comparable engine performance and combustion as compared to diesel fuel. In addition, it was reported that the biodiesel fuels have demonstrated a better tribological performance than the diesel fuels [15]. Even though non-edible oils have the potential as an alternative to edible oil, they are yet to reach commercial scales for feedstock production. As a comparison, palm oil yielded an average 4000–5000 kg/hectare/year, while oil yielded for jatropha and karanja is less than 2500 kg/hectare/year [16]. With this consideration, palm oil was chosen in the present study.

Recently, new light biofuels such as eucalyptus, pine, and camphor oils have been studied by a few researchers as a new source of biofuels [17–19]. In contrast to SVO, these light biofuels have relatively lower viscosity and high volatility. Unlike SVO, which is produced from the seed or kernel, eucalyptus oil is obtained mostly by a steam distillation process of leaves and twigs of the plants (*Eucalyptus globulus*) while camphor oil is extracted by steam from the chipped wood of the camphor tree (*Cinnamomum camphora*). Meanwhile, pine oil is derived from the resin of the pine tree (*Pinus sylvestris*).

Back in 1981, Hoki et al. [20] studied various gasoline–eucalyptus oil blends on engine performance. They found that the performance of blended fuel is similar to gasoline fuel. Blended fuel also provides better anti-knocking compared to gasoline, due to its high octane number. Later, Poola et al. [21] found that a blend of 20% eucalyptus oil with gasoline provides better engine performance than gasoline fuel at a higher compression ratio. Hydrocarbons and carbon monoxide were also found to be lower compared to gasoline fuel. Despite eucalyptus oil being tested on a spark ignition engine, Devan and Mahalakshmi [22] studied a blend of paradise oil methyl ester and eucalyptus oil as the fuels for a diesel engine. Notable reductions of CO, HC, and smoke, but a slight increase of NO_x emission compared to diesel fuel, were observed. The blend of 50% eucalyptus oil exhibited similar performance to that of diesel fuel. A blend of camphor oil [18] and pine oil [23] has also been reported to produce better performance, combustion, and emission characteristics. Recently, a blend of eucalyptus oil with palm kernel methyl ester has been reported to enhance engine performance and reduce certain emissions, especially at high load conditions [24].

In the present study, a new light biofuel—Melaleuca Cajuputi oil (MCO)—has been introduced and blended with refined palm oil (RPO) as a strategy to reduce the viscosity, density, and enhance the volatility of the blend. MCO is highly volatile and has low viscosity as compared to RPO, which has relatively low volatility and very high viscosity. The physicochemical characteristics of RPO-MCO blends are analyzed and compared to ASTM 6751/EN 14214 standards to see its potential as a new source of biofuel. In this study, a regression analysis method was employed to determine the optimal blend ratio. The optimized blend is further tested on a single cylinder diesel engine to investigate its performance, combustion, and emission characteristics.

Overview of Melaleuca Cajuputi Oil and Refined Palm Oil

Melaleuca cajuputi is a local tree species found in northern Australia, Indonesia, Malaysia, Thailand, Vietnam, Cambodia, and Papua New Guinea. Different terms are used in different countries to refer to the *Melaleuca cajuputi* tree, such as Kayu Putih (Indonesia) and Gelam (Malaysia). The Cajuputi

(also spelt cajuput or cajeput) is possibly referring to the Indonesian name for the tree [25,26]. *Melaleuca Cajuputi* oil (MCO) is categorized as an essential oil commercially used as a home remedy for stomach aches, headaches, colds, and relief of itching caused by insect or mosquito bites [26]. Trees of these species can typically reach up to 25 m in height. Figure 1 shows the tree and leaves of *Melaleuca cajuputi* while Figure 2 shows the neat MCO and refined palm oil (RPO). The world production of MCO is estimated to be more than 600,000 kg annually where Indonesia and Vietnam produce more than half of the total oil. Indonesia is estimated to produce more than 350,000 kg of oil annually, and Vietnam produces an average of 100,000 kg of oil per year [27,28]. This oil is extracted from the leaves and twigs mostly through water-steam distillation. This extraction method is cheap, simple, and not hazardous. An alternative process, like supercritical fluid extraction, is seldom used because it is more expensive compared to the water-steam distillation process. Figure 3 shows the schematic diagram of the water-steam distillation method to extract MCO.

This oil is a complex mixture of volatile components extracted from the leaves and twigs through water-steam distillation. MCO can be divided into two main groups which are monoterpenes (monoterpenes hydrocarbon and oxygenated monoterpenes) and sesquiterpenes (sesquiterpenes hydrocarbon and oxygenated sesquiterpenes) [29]. As previously reported, the major constituent of MCO is 1,8-cineole comprising 30% to 70% of the oil [25,30]. In addition, MCO comprises lipophilic compound; this lipophilicity property enhances MCO solubility in SVOs and a wide range of liquid hydrocarbons without the presence of a surfactant [26].

Refined palm oil (RPO) is a product from the fractionation process of crude palm oil, which has better flow properties compared to crude oil. In general, crude palm oil is a semi-solid fat at temperatures lower than 20 °C. Palm oil was chosen in this study because of its abundantly available feedstock and some of its properties are similar to diesel fuel [31]. In comparison, palm oil yields the highest oil compared to soybean, sunflower, rapeseed, or even other non-edible vegetable oils. Palm oil can produce an average of 4 to 5 tons of oil every year for every hectare of land [32]. The high yield of palm oil is making it a promising feedstock for an alternative biofuel. Despite numerous research conducted on non-edible oils, those non-edible oils are still unable to compete with palm oil in terms of oil yielded.

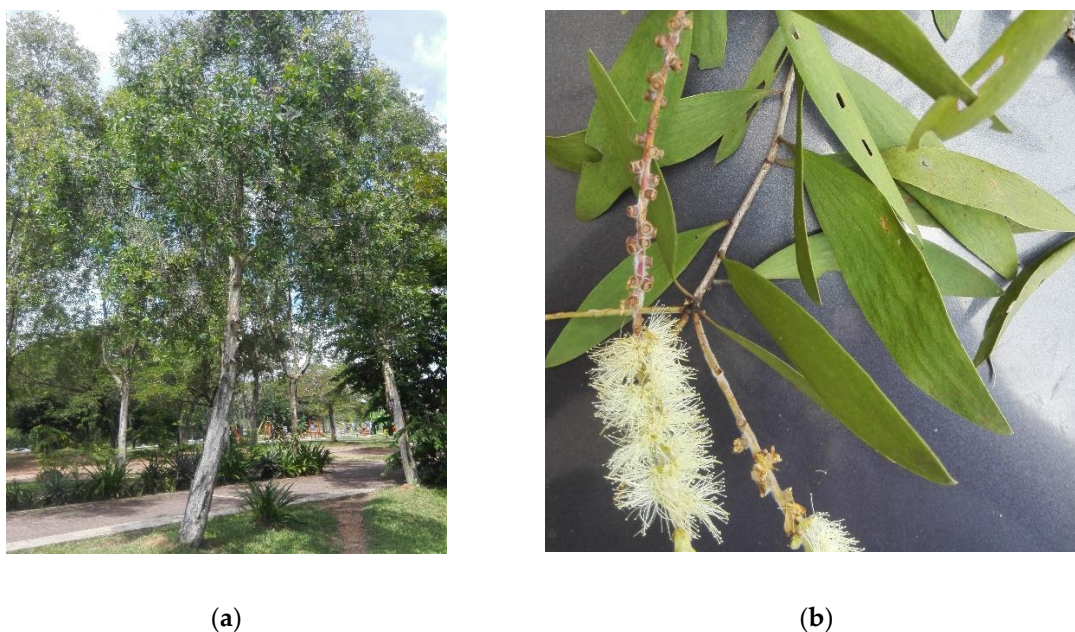


Figure 1. (a) *Melaleuca cajuputi* tree and (b) *Melaleuca cajuputi* leaves.

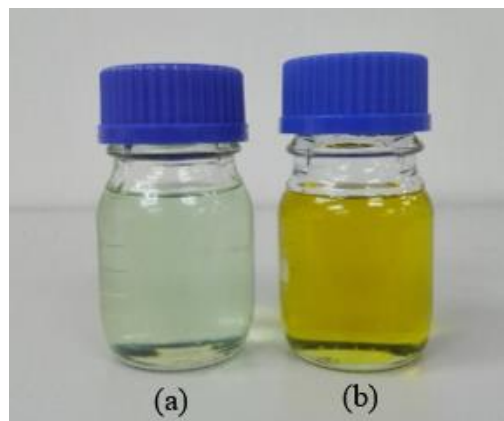


Figure 2. (a) Melaleuca Cajuputi oil and (b) refined palm oil.

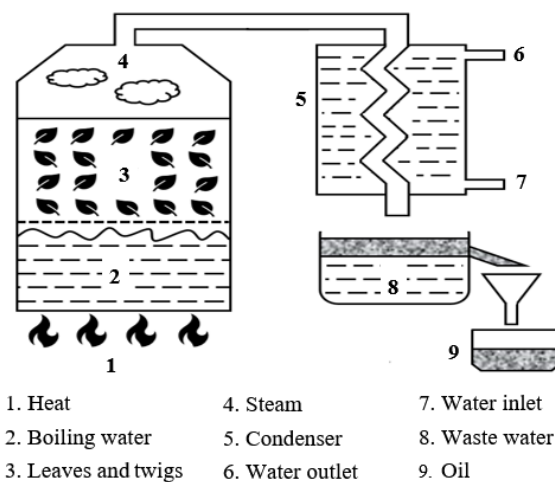


Figure 3. Water-steam distillation method.

2. Materials and Methods

2.1. Materials

Melaleuca Cajuputi oil (MCO) used in this study was purchased from a local supplier who imports it from Indonesia. In Indonesia, most of the Cajuputi trees are found in the Maluku islands. MCO is highly volatile and has a clear greenish color. Meanwhile, the refined palm oil (RPO) used was purchased from the local market.

2.2. Hybrid Biofuel Preparation

Hybrid biofuel of RPO-MCO blends was prepared on a volume basis (v/v). Two samples of straight oil of 100% RPO and 100% MCO, as well as three blends at a mixing ratio of 25% (MCO25RPO75), 50% (MCO50RPO50), and 75% (MCO75RPO25) MCO with RPO, were prepared. Due to MCO's lipophilicity property, it is able to blend with RPO at any ratio without the presence of a surfactant [26]. This advantage leads to simplicity of the blend at minimum cost and fast preparation. Each blend was homogeneously mixed with a magnetic stirrer. The gravitational stability test [33] was conducted for a month to observe any signs of phase separation. A stable blend is important to ensure the quality of the fuel and make it commercially usable.

2.3. Physicochemical Properties Analyses

The kinematic viscosity of RPO, MCO, and their blends were measured according to American Society for Testing and Materials (ASTM) D445. Calibrated glass capillary viscometer (Cannon-Fenske

viscometer) was used to measure the viscosity values at 40 °C. Kinematic viscosity was obtained by multiplying the time taken for MCO flowing to pass through a viscometer with the tube constant provided by the manufacturer.

The density was obtained by dividing mass over the volume of the biofuel sample. The volume was measured using a 25 mL Gay-Lussac pycnometer at an ambient temperature (27 °C) and weighed using a high precision Shimadzu ATX224 analytical balance. The pycnometer used was certified according to ISO 3507.

The calorific value was measured according to ASTM D240. An adiabatic oxygen bomb calorimeter (Nenken 1013-B, Japan) was used to measure the energy available from the biofuel.

RPO fatty acids and MCO constituents were analyzed using the Perkin Elmer, Clarus 600 gas chromatography mass spectrometry (GC-MS). The GC-MS used helium gas as a carrier with a column size of 30 m × 250 µm. The initial temperature was 50 °C and then increased to 230 °C at 3 °C/min. The chemical compositions were confirmed by comparing their retention times and mass spectra with data from library databases and published literature.

The flash point value was measured according to ASTM D3828. A closed cup flash tester (K16500, Koehler instrument company, USA) was used to measure the flash point value of the MCO.

The acid value of MCO was measured according to ASTM D664. A 785 DMP Titrino (Metrohm, Switzerland) was used to measure the amount of acidic substance in the oil. Generally, a high acid value will cause corrosion to the fuel system and parts of the internal combustion engine.

The water content of MCO was measured according to European Standards (EN) 12937 and carried out on a 787 Karl Fisher titrator (Metrohm, Switzerland). High water content will likely promote the corrosion of the engine parts and injection system.

Boiling point was determined using the Melting Point M-565 (BUCHI, Switzerland). The measurement method was performed according to the manufacturer's standard.

2.4. Hybrid Biofuel Optimization and Selection

In the present study, a high viscosity RPO and low viscosity MCO were used to formulate a hybrid biofuel, aiming to study its potential as a new source of biofuel. This hybrid biofuel is totally 100% neat oil, which does not include any biodiesel or fossil fuel in its preparation. Somehow, at present, there is no specific biofuel standard for such a blend. Therefore, in this work, the newly developed hybrid biofuel will be benchmarked against the ASTM D6751/EN 14214 standards as guidelines. It is renowned that RPO is the promising biofuel alternative to fossil diesel. However, the main reasons why RPO cannot directly be used as diesel engine fuel are its relatively high viscosity and density, which lead to poor atomization, low volatility, and excessive carbon deposit inside the combustion chamber in the long term. Thus, in this study, only the selected and optimized hybrid biofuel blend will be chosen to be tested on a diesel engine to investigate its performance and emission characteristics.

Obviously, viscosity and density have enormous influence on fuel spray characteristics, fuel atomization, flow properties, engine performance, and exhaust emissions [34–36]. Therefore, in this study, these two key properties were thoroughly optimized to meet the ASTM D6751/EN 14214 standards before the fuel was introduced to the engine.

The data of physicochemical properties were analyzed using the regression method to generate a mathematical model that presented the correlation between blending ratio and its effect on viscosity or density. The mathematical model obtained was used to predict the optimum blend proportion for a desirable viscosity and density according to ASTM D6751/EN 14214. This optimization method was very beneficial to expedite the experiment and reduce cost and waste of materials compared to the trial and error experiment.

2.5. Experimental Setup and Measurement Procedure

In this study, a single-cylinder air-cooled four-stroke diesel engine manufactured by Yanmar (Italy) was used for the experiment. The specifications of the engine are tabulated in Table 1. The engine

was coupled to the 20 kW eddy current dynamometer to measure the brake torque and brake power. The fuel mass consumption was measured using an electronic scale with a 0.1 gram accuracy. In order to measure the air flow rate, a mass air flow sensor (hot wire type) was used. In addition, the exhaust gas temperature was measured using a K-type thermocouple.

The in-cylinder pressure was measured using a Kistler 6051A piezoelectric pressure transducer mounted at the top of the cylinder head and the signal was transmitted to a Kistler 5027A12 charge amplifier. Furthermore, the crankshaft rotation angle was measured using an incremental type rotary encoder.

In this study, the exhaust emissions and smoke opacity were measured using a SPTC Autocheck (Korea) emissions and smoke analyzer. The emissions analyzer measured nitrogen oxides (NO_x) at a range of 0–5000 ppm, hydrocarbon (HC) at a range of 0–10,000 ppm, carbon monoxide (CO) at a range of 0–10% vol., carbon dioxide (CO_2) at a range of 0–20% vol., and oxygen (O_2) at a range of 0–25% vol. Meanwhile, the smoke analyzer measured smoke opacity at a range of 0–100% with a resolution of 0.1%.

In this work, only optimized hybrid biofuel which has the viscosity and density that meet ASTM D6751/EN 14214 standards was selected for the engine test and compared with the baseline diesel fuel. The experiment was performed at the wide-open throttle (WOT) with engine speed ranging from 2000 to 3500 rpm. Before the experiment started, the engine was initially running for 10 minutes to allow the engine to attain the optimum operating condition. For in-cylinder pressure measurement, 100 continuous engine cycles were recorded, and the average pressure trace was calculated. The schematic diagram of the experimental setup is presented in Figure 4.

Table 1. Engine specifications.

Model/Make	Yanmar L70N
Fuel injection system	Direct injection
Maximum output (kW)	4.9
Rated speed (rpm)	3600
Displacement (litre)	0.320
Bore × stroke (mm)	78 × 67
Cylinder	single
Compression ratio	20:1
Cooling system	Forced air
Lubrication system	Forced lubricating

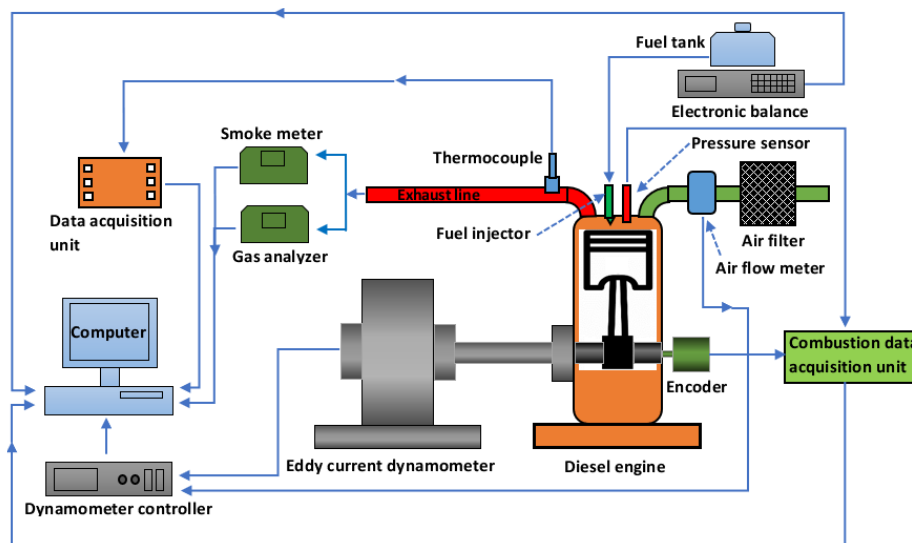


Figure 4. Schematic diagram of engine dynamometer setup.

3. Results

3.1. Gravitational Stability Test

All the blends were kept in bottles and stored at ambient temperature for a month. The blends were visually observed, and no sign of separation occurred during the test period. The blends also remained as one-phase clear and transparent liquid. Thus, the blends were considered highly stable and suitable for long-term storage and transportation. Figure 5 shows the appearance of blended fuels after being stored for one month.

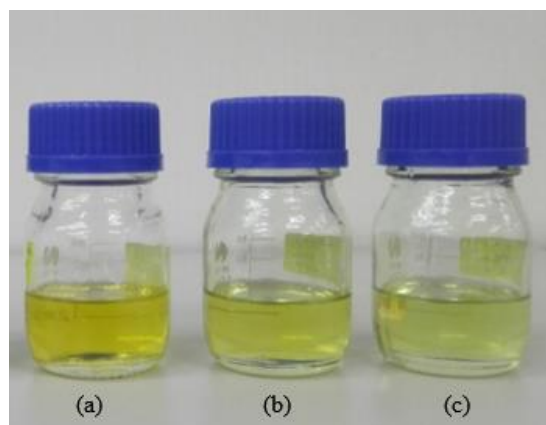


Figure 5. Appearance of hybrid biofuel after a month. (a) MCO25RPO75; (b) MCO50RPO50; (c) MCO75RPO25.

3.2. Chemical Constituent of *Melaleuca Cajuputi* Oil

Figure 6 presents the chromatogram of *Melaleuca Cajuputi* oil (MCO). Meanwhile, Table 2 lists the relative content of the main composition from MCO expressed as the percentage from the total area obtained from the gas chromatography mass spectrometry (GC-MS) analysis. Overall, there were 35 compounds (96.6% of the total oil) identified. Hydrocarbon is the major group at 64.8% and oxygenated product at 34.6%. Under oxygenated products, seven alcohols were identified to represent 6.8% of the total oil. The presence of alcohol is important for its antibacterial properties [37], and to enhance the volatility of the oil. The high compound of hydrocarbons (HC) and the presence of alcohols are possibly the reasons for the high calorific value (CV) of MCO compared to that of diesel fuel. The high compound of HC also indicated that MCO is a potential source of biofuel [38].

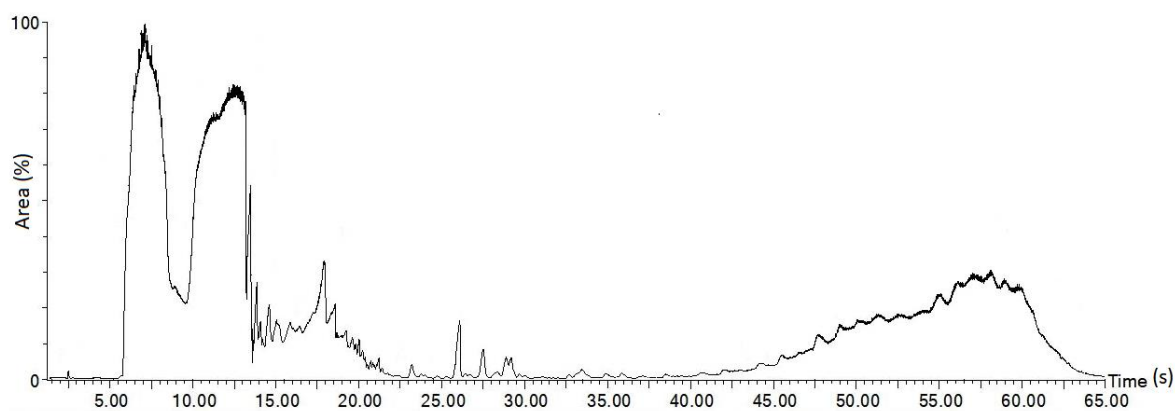


Figure 6. Chromatogram of *Melaleuca Cajuputi* oil.

Table 2. List of compounds identified by gas chromatography mass spectrometry (GC-MS) analysis.

No.	Compound	Chemical Class	Molecular Formula	Composition (%)
1	α -Pinene	hydrocarbon	C ₁₀ H ₁₆	26.12
2	1,8-Cineole	oxygenated product (ether)	C ₁₀ H ₁₈ O	27.66
3	γ -Terpinene	hydrocarbon	C ₁₀ H ₁₆	1.23
4	Terpinolene	hydrocarbon	C ₁₀ H ₁₆	0.38
5	Undecane	hydrocarbon	C ₁₁ H ₂₄	0.15
6	Trans-decalin, 2-methyl-	hydrocarbon	C ₁₁ H ₂₀	0.31
7	Trans-9-methyldecalin	hydrocarbon	C ₁₁ H ₂₀	0.40
8	1-Isopropenyl-4-methyl-1,2-cyclohexanediol	oxygenated product (alcohol)	C ₁₀ H ₁₈ O ₂	0.53
9	Naphthalene, decahydro-2,3-dimethyl-	hydrocarbon	C ₁₂ H ₂₂	0.35
10	1-Menthol	oxygenated product (alcohol)	C ₁₀ H ₂₀ O	2.49
11	α -Terpineol	oxygenated product (alcohol)	C ₁₀ H ₁₈ O	0.87
12	Verbenol	oxygenated product (alcohol)	C ₁₀ H ₁₆ O	0.36
13	Cyclohexane, (4-methylpentyl)-	hydrocarbon	C ₁₂ H ₂₄	0.37
14	6-Methyltridecane	hydrocarbon	C ₁₄ H ₃₀	0.24
15	Undecane, 2,3-dimethyl-	hydrocarbon	C ₁₃ H ₂₈	0.11
16	Dodecane, 2-methyl-6-propyl-	hydrocarbon	C ₁₆ H ₃₄	0.13
17	Undecane, 2,9-dimethyl-	hydrocarbon	C ₁₃ H ₂₈	0.11
18	Tridecane	hydrocarbon	C ₁₃ H ₂₈	0.08
19	α -Terpinyl acetate	oxygenated product (acetate)	C ₁₂ H ₂₀ O ₂	0.10
20	Ylangene	hydrocarbon	C ₁₅ H ₂₄	0.02
21	β -Caryophyllene	hydrocarbon	C ₁₅ H ₂₄	0.44
22	α -Caryophyllene	hydrocarbon	C ₁₅ H ₂₄	0.24
23	Longifolene-(v4)	hydrocarbon	C ₁₅ H ₂₄	0.07
24	β -Selinene	hydrocarbon	C ₁₅ H ₂₄	0.20
25	α -Selinene	hydrocarbon	C ₁₅ H ₂₄	0.17
26	α -Bergamotene	hydrocarbons	C ₁₅ H ₂₄	0.03
27	δ -Cadinene	hydrocarbon	C ₁₅ H ₂₄	0.03
28	Caryophyllene oxide	oxygenated product	C ₁₅ H ₂₄ O	0.03
29	Viridiflorol	oxygenated product (alcohol)	C ₁₅ H ₂₆ O	0.17
30	β -Eudesmol	oxygenated product (alcohol)	C ₁₅ H ₂₆ O	0.06
31	Sulfurous acid, butyl heptadecyl ester	others	C ₂₁ H ₄₄ O ₃ S	0.16
32	Tetradecane, 2,6,10-trimethyl-	hydrocarbon	C ₁₇ H ₃₆	1.50
33	1-Hexadecanol, 2-methyl-	Oxygenated product (alcohol)	C ₁₇ H ₃₆ O	2.32
34	17-Pentatriacontene	hydrocarbon	C ₃₅ H ₇₀	6.33
35	Tetratetracontane	hydrocarbon	C ₄₄ H ₉₀	25.85
Class compositions				
Hydrocarbons				64.8
Oxygenated products				34.6
Others				0.2
Total composition				99.6

Individually, the main components of MCO are 1,8-cineole (27.7%), α -pinene (26.1%), and tetratetracontane (25.9%). The cyclic ether 1,8-cineole, has high stability and low chemical reactivity which make it resistant to polymerization, oxidation, and thermal decomposition [22]. It is reported that the blend of eucalyptus oil (which is rich in 1,8-cineole) either with gasoline or biodiesel has enhanced the performance and exhaust emissions of the engine [21,22,39]. Thus, sole or blended MCO with other fuels is expected to provide reliable engine performance and exhaust emissions.

3.3. Basic Physicochemical Properties of RPO-MCO Blends

The properties of biofuel are important to ensure the suitability of the oil before being introduced to the engine. The basic properties of MCO, RPO, and their blends are presented in Table 3. The kinematic viscosity of MCO was 2.2 mm²/s, which is comparable to diesel fuel, yet significantly lower compared to those of vegetable oils. Mostly, vegetable oils either edible or non-edible have viscosity in the range of 25–40 mm²/s. The low viscosity suggests that MCO will offer a good flow property, especially during cold weather. MCO density was determined at 869 kg/m³ which was within the range of diesel. Viscosity and density are the well-known factors that have significant effects on fuel atomization and injection spray characteristics. MCO, having low viscosity and density, is expected to provide a decent quality of spray characteristics and enhance fuel atomization for a better air fuel mixture. Notably, the amount of energy (CV) obtained from MCO is comparable to that of diesel fuel. High CV is important to provide good engine thermal efficiency and reduce fuel consumption. The flash point of MCO was 50 °C, which is mostly similar to diesel fuel. Its low flash point value indicated that MCO is a volatile oil, which is important for fuel atomization. However, water content and acid value of the oil were high compared to the ASTM 6751 standard. The high moisture and acid content could lead to corrosion of certain parts of the engine and fuel system.

On the other hand, the kinematic viscosity of RPO was significantly higher compared to the maximum limit of ASTM D6751/EN 14214. The high viscosity of RPO comes from triglycerides that contain three fatty acids and one glycerol. The fatty acid composition of RPO is presented Table 4. The major compositions identified were oleic and palmitic acid at 49% and 32.6%, respectively. Specifically, high content of oleic acid contributes to a good oxidative stability [40]. However, high content of oleic acid contributes to high density of RPO [41]. The high viscosity and density are the main reasons that limit its potential as engine fuel. High viscosity and density will increase the fuel impingement with cylinder wall and piston due to longer fuel spray penetration. Impingement would lead to the formation of carbon deposit and higher unburnt hydrocarbon emissions.

Notably, the strategy to blend high viscosity RPO with low viscosity MCO successfully reduced the viscosity and density of hybrid biofuel. The higher the fraction of MCO, the lower the viscosity and density of the blends observed. The blend of RPO25MCO75 was found to have viscosity and density levels within the ASTM/EN standards. In addition, the calorific value of the blend was also close to diesel, which is important to provide good combustion efficiency. It was observed that all the blends exhibited lower flash points, similar to the diesel range. The flash point value describes the tendency of the fuel to initiate flash and start the flame. The higher the MCO fraction in the blends, the lower the flash point values obtained. The blends also obtained lower boiling points which could enhance the atomization and evaporation of the fuel.

Table 3. Physicochemical properties of neat and blends of refined palm oil-Melaleuca Cajuputi oil (RPO-MCO).

Property	ASTM D6751	EN 14214	Diesel	RPO25 MCO75	RPO50 MCO50	RPO75 MCO25	RPO32 MCO68	RPO	MCO
Kinematic viscosity at 40 °C (mm ² /s)	1.9–6.0	3.5–5.0	3.4	4.6	9.6	19.0	5.45	42	2.2
Density (kg/m ³)	880	860–900	835	878.2	887.1	895.98	880.20	905.5	871.4
Calorific value (MJ/kg)	-	35	44.8	42.3	41.5	40.8	42.1	40.3	43.2
Flash point (°C)	100–170	>120	50–55	51–52	53–55	65–67	52–53	210–215	50–51
Boiling point (°C)	-	-	150–343	134	141	189	135	>250	121
Water content (vol. %)	Max. 0.05	-	-	0.31	0.33	0.43	0.32	0.56	0.28
Acid value (mg KOH/g)	Max. 0.5	Max. 0.5	-	0.55	0.69	0.89	0.60	7.28	5.52

Table 4. Fatty acid composition of RPO.

Fatty Acid	Mol. Formula	Composition (%)
Lauric	C ₁₂ H ₂₄ O ₂	2.4
Myristic	C ₁₄ H ₂₈ O ₂	1.2
Palmitic	C ₁₆ H ₃₂ O ₂	32.6
Stearic	C ₁₈ H ₃₆ O ₂	2.9
Oleic	C ₁₈ H ₃₄ O ₂	49
Linoleic	C ₁₈ H ₃₂ O ₂	11.9

Even though the blend of RPO25MCO75 successfully achieved the viscosity and density within the ASTM D6751/EN 14214 standards, the present work targeted to obtain the blend that has the highest RPO percentage but still obtain viscosity and density levels within the allowable limits. Thus, further optimization analysis was carried out to select the optimum blend ratio.

3.4. Optimization of Hybrid Biofuel

To predict and select the optimum blend ratio, the regression analysis method was employed. This method developed the mathematical model of correlation between the blends' fraction and their effect on the viscosity and the density. Figure 7 shows the correlation between the MCO fraction and viscosity obtained from the experimental data. From the regression analysis, the following mathematical equation was proposed:

$$v = 41.135e^{-0.029x} \quad (1)$$

where v is kinematic viscosity (mm²/s) and x is volume fraction of MCO in the blend. The exponential regression obtained high R² value of 0.9996 which shows a good fit of regression trend line with the measured data.

Meanwhile, the correlation between MCO fraction and density is shown in Figure 8. From the tabulated data, linear regression with R² of 0.9967 is the best fit to describe the correlation of MCO fraction and density of the blends. The mathematical equation of the correlation is given by:

$$\rho = -0.3439x + 904.83 \quad (2)$$

where ρ is density (kg/m³) and x is volume fraction of MCO in the blend.

The optimization was performed based on the mathematical equations obtained from the regression analysis. The goal of the optimization was set to maximize the fraction of RPO in the blend and the desirable viscosity and density within the ASTM D6751/EN 14214 requirements. From the evaluation of Equations (1) and (2), the optimum blend ratio of RPO32MCO68 was suggested. The predicted kinematic viscosity and density obtained are 5.7 mm²/s and 881.44 kg/m³, respectively. To evaluate the accuracy of the predicted values obtained, the measured data were compared to the calculated data. The comparison and the discrepancy between measured and calculated data were tabulated in Table 5. Notably, the discrepancy is less than 5% which indicates that the mathematical models obtained were reliable to predict the viscosity and density of the RPO-MCO blends. Therefore, the blend ratio of RPO32MCO68 was selected to further analyze its performance and emissions on a diesel engine.

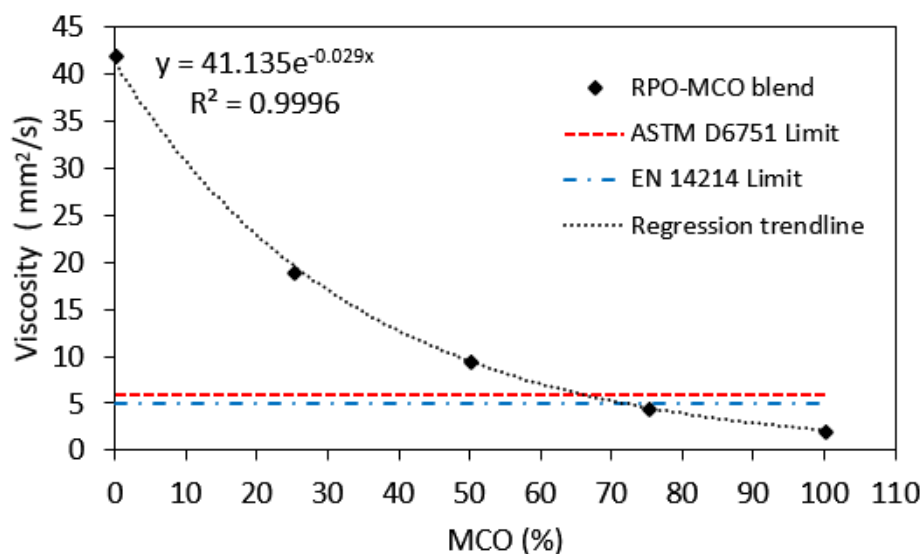


Figure 7. Correlation between MCO fraction and viscosity.

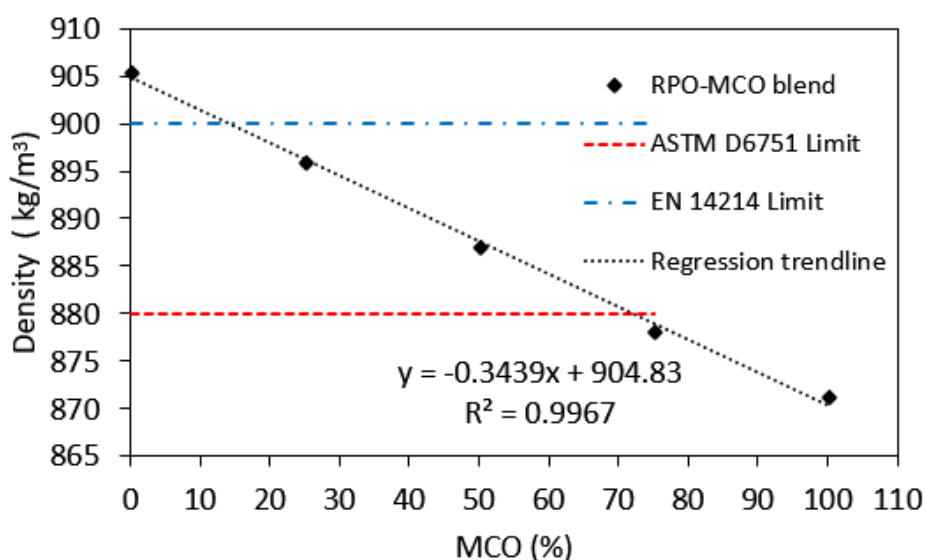


Figure 8. Correlation between MCO fraction and density.

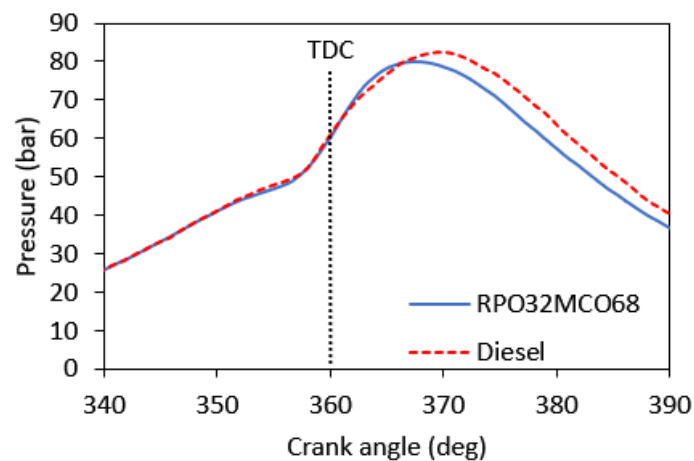
Table 5. Comparison between measured and calculated data of viscosity and density.

Blend (vol. %)	Kinematic Viscosity (mm ² /s)		Discrepancy (%)	Density (kg/m ³)		Discrepancy (%)
	Measured	Calculated		Measured	Calculated	
RPO25MCO75	4.60	4.70	2.2	878.20	879.04	0.10
RPO50MCO50	9.60	9.70	1.0	887.10	887.64	0.10
RPO75MCO25	19.0	19.90	4.7	895.98	896.23	0.03
RPO32MCO68	5.45	5.70	4.6	880.20	881.44	0.14

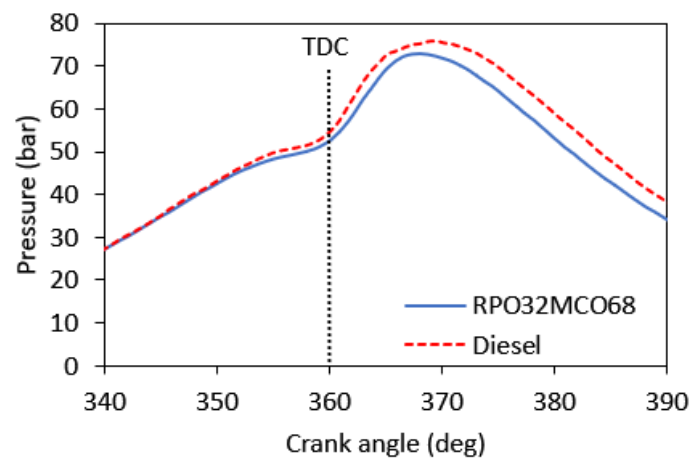
3.5. Combustion Analysis

The comparison of in-cylinder pressure between optimized hybrid biofuel (RPO32MCO68) and baseline diesel fuel at various engine speeds is presented in Figure 9. The pressure curves plotted were the average of 100 consecutive combustion cycles. It can be observed that an engine running on hybrid biofuel had a slightly lower peak pressure at low and medium engine speeds. However, at high engine speeds, the peak pressure differences between hybrid biofuel and diesel became larger. At the engine speed of 2000 rpm, peak cylinder pressure of the RPO32MCO68 blend occurred earlier than diesel fuel. Notably, the peak cylinder pressure of the blend was found to be 80.0 bar at 367.4° after top dead

center (ATDC), while the peak cylinder pressure obtained for baseline diesel fuel was 82.4 bar at 369.5° ATDC. The pressure difference was about 2.9% as compared to diesel fuel. At 2500 rpm, it was found that the peak pressure for baseline diesel was 76.0 bar at 369.6° ATDC, meanwhile, the RPO32MCO68 biofuel blend obtained peak pressure of 73.1 bar at 368.1° ATDC. The drop in peak pressure was about 3.8%. As the engine speed increased to 3000 rpm, the peak cylinder pressure for baseline diesel was 71.6 bar at 371° ATDC and 69.7 bar at 369.5° for the RPO32MCO68 biofuel blend. The pressure reduction was about 2.7%. Upon further increase of engine speed to 3500 rpm, the peak cylinder pressure for baseline diesel was recorded at 69.1 bar at 370.3° ATDC, while the peak cylinder pressure for the RPO32MCO68 blend was recorded at 61.7 bar at 371.6° ATDC. The difference in pressure was about 10.7%. At all ranges of testing, the in-cylinder pressure of hybrid biofuel (RPO32MCO68) is slightly lower as compared to baseline diesel fuel. This is probably due to lower calorific value of hybrid biofuel which leads to lower heat release during the combustion process. In addition, hybrid biofuel has a slightly higher viscosity and density compared to diesel fuel, and has contributed to poor fuel atomization and low combustion efficiency, which reduces the in-cylinder peak pressure. Generally, for both fuels, the peak cylinder pressure decreases as the engine speed increases. From the analysis, it was found that the RPO32MCO68 blend has shown remarkable peak cylinder pressure close to the baseline diesel. Taking into consideration that this blend involved only two neat biofuels, the results obtained are quite impressive.

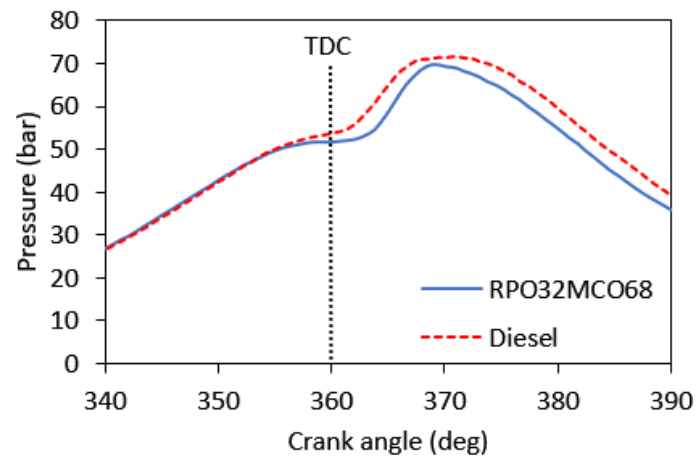


(a)

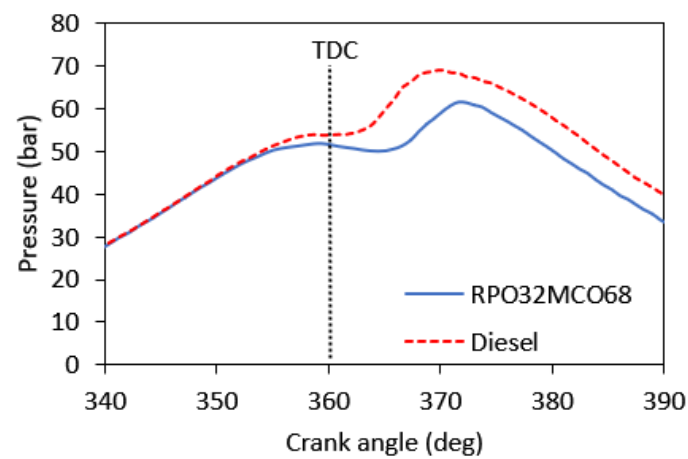


(b)

Figure 9. Cont.



(c)



(d)

Figure 9. Cylinder pressure versus crank angle degree for tested fuels at (a) 2000 rpm; (b) 2500 rpm; (c) 3000 rpm, and (d) 3500 rpm.

3.6. Performance Analysis

3.6.1. Engine Torque

Figure 10 shows the engine torque variation as a function of the engine speed for the RPO32MCO68 hybrid biofuel blend and baseline diesel fuel. The torque values for both fuels decreased with the increase in the engine speed. The maximum torque was at 2000 rpm and then gradually decreased as the engine speed increased afterwards. The range of test for the RPO32MCO68 blend demonstrated a comparable engine torque to that of diesel fuel except for at 3500 rpm. At maximum engine speed, torque for RPO32MCO68 was found to be 21.4% lower compared to baseline diesel fuel. Lower torque at maximum speed is associated with the low peak pressure obtained during the combustion process. This can be related to the fact that the RPO32MCO68 blend has lower CV compared to the baseline diesel. In addition, the RPO32MCO68 blend also had slightly higher viscosity which affected fuel atomization, thus leading to low combustion efficiency and in-cylinder peak pressure [42].

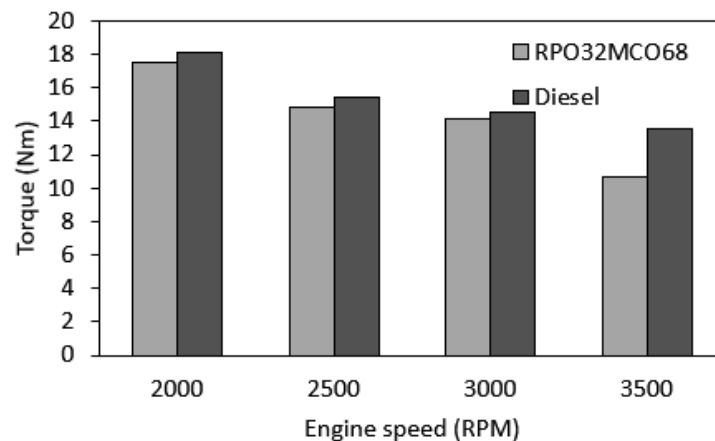


Figure 10. Comparison of engine torque as a function of engine speeds.

3.6.2. Engine Brake Power

The engine brake power as a function of engine speed for all tested fuels is presented in Figure 11. At the whole range of speed, the brake power produced from the RPO32MCO68 biofuel was slightly lower compared to baseline diesel fuel. The brake power reductions were 3.42%, 4.2%, 2.62%, and 20.6% at 2000, 2500, 3000, and 3500 rpm, respectively. Notably, the largest brake power reduction for the RPO32MCO68 blend was recorded at the maximum engine speed. The possible explanation for this result is related with the lower engine torque as discussed earlier. Despite lower brake power at 3500 rpm, interestingly, the RPO32MCO68 blend recorded a comparable brake power compared to the baseline fuel at lower engine speed.

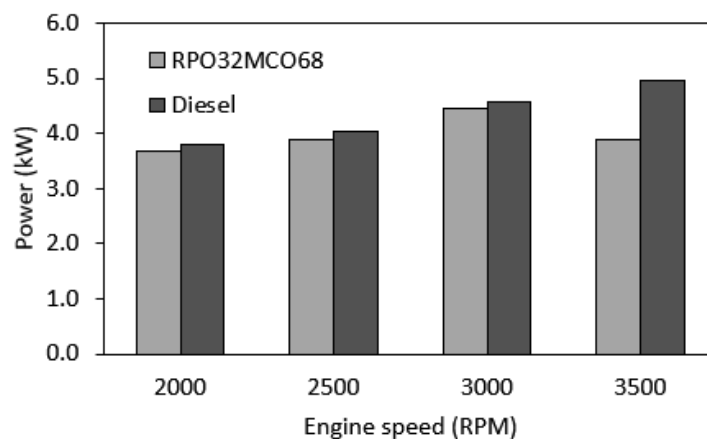


Figure 11. Comparison of engine power as a function of engine speeds.

3.6.3. Brake Specific Fuel Consumption

Figure 12 compares the experimental data of brake specific fuel consumption (BSFC) for RPO32MCO68 and baseline diesel fuel. BSFC is an important parameter to compare the fuel efficiency of different tested fuels. It is apparent that the RPO32MCO68 blend recorded a slightly higher BSFC than diesel fuel at the entire range of engine speeds. The BSFC increments were 3.3%, 6.6%, 7.5%, and 6.5% at 2000, 2500, 3000, and 3500 rpm, respectively. Comparing the two results, it can be seen that there was no significant increase in RPO32MCO68 BSFC as compared to baseline diesel fuel where the maximum increment was only 7.5%. Higher BSFC obtained by the RPO32MCO68 blend was mainly due to lower CV where more fuel was required to combust in order to retain the same engine speed.

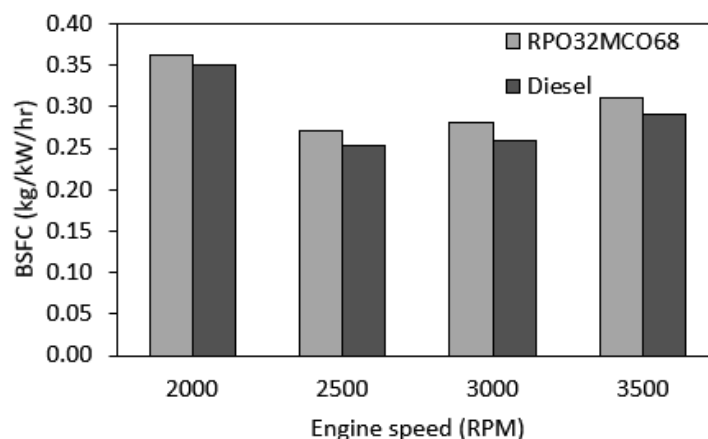


Figure 12. Comparison of brake specific fuel consumption (BSFC) as a function of engine speeds.

3.7. Emissions Analysis

3.7.1. NO_x Emission

Figure 13 shows the variation of NO_x emission for the RPO32MCO68 blend in comparison to baseline diesel fuel. High NO_x formation was mainly related to the high combustion temperature. The graph shows that both fuels exhibited a similar trend where the NO_x was low at low engine speed, significantly increased at medium speed, and gradually decreased toward high engine speed. Notably, at the entire range of test, the RPO32MCO68 blend produced lower NO_x as compared to baseline diesel fuel. The NO_x reductions were 3.9%, 3.5%, 7.7%, and 17.3% at 2000, 2500, 3000, and 3500 rpm respectively. This reduction was possibly because of lower heat released during the combustion process due to low CV [43]. Furthermore, slightly high viscosity of the blend also contributed to low combustion temperature in comparison to baseline diesel.

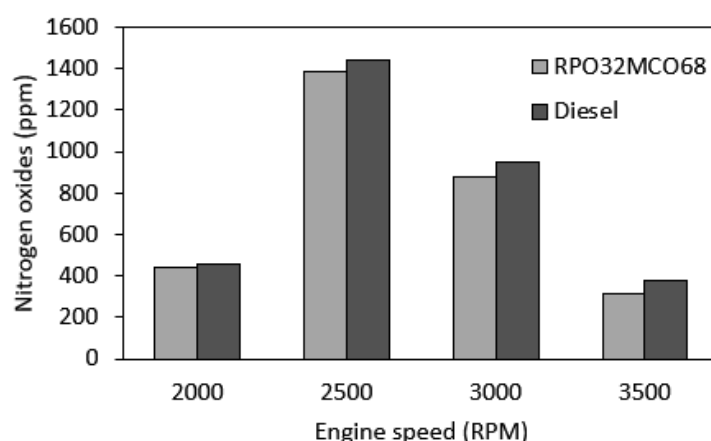


Figure 13. Comparison of nitrogen oxide emission as a function of engine speeds.

3.7.2. CO Emission

The CO emission as a function of engine speed for tested fuel is presented in Figure 14. CO emission is mainly formed when there is lack of oxygen to react with the carbon to form CO₂. As can be seen in Figure 14, at all range of engine speeds, the CO emission of the RPO32MCO68 blend slightly surpassed the baseline diesel fuel. CO was high at low speed and progressively decreased as the engine speed increased. Relatively high CO at low engine speed was mainly due to the engine operating at rich air-fuel mixture, where more fuel was injected but there was less oxygen to react. Moreover, incomplete combustion due to non-homogenized air-fuel mixture also led to the formation

of CO [43]. As the engine speed increased, more oxygen was introduced into the combustion chamber, which allowed the engine to operate at lean mixture, thus reducing CO emission.

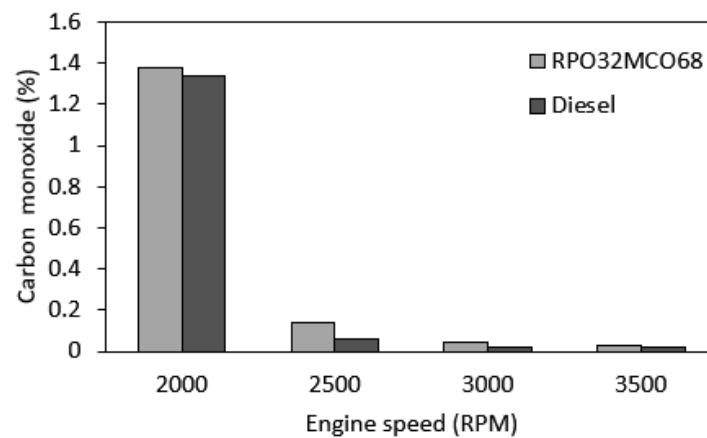


Figure 14. Comparison of carbon monoxide emission as a function of engine speeds.

3.7.3. HC Emission

HC emission is the product of incomplete combustion due to fuel properties, fuel spray characteristics, and engine operating conditions. Figure 15 shows the HC emission variation as a function of the engine speed for the RPO32MCO68 hybrid biofuel blend and baseline diesel fuel. At the entire range of engine speeds, the HC emission of the RPO32MCO68 blend was higher compared to the baseline diesel fuel. The emission was higher at 2000 rpm but gradually decreased as engine speed increased. A possible explanation for these results may be due to high viscosity and poor fuel atomization of blended fuel. Poor fuel atomization formed a non-uniform air-fuel mixture, thus causing some of the fuel being unable to combust. Another possible explanation is the occurrence of fuel impingement with the cylinder wall and piston head due to excessive spray penetration [6]. High viscosity and density caused large droplets and longer spray penetration compared to baseline diesel fuel. In addition, blended fuel contains lower cetane numbers than diesel fuel, causing longer ignition delay and a shorter combustion period, thus leading to higher HC emission being produced.

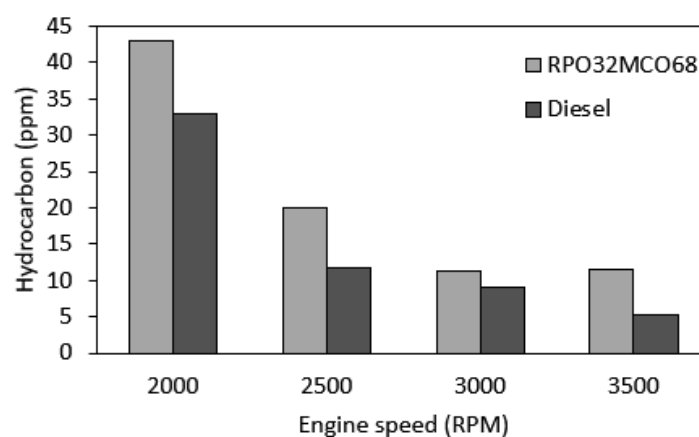


Figure 15. Comparison of unburned hydrocarbon emission as a function of engine speeds.

3.7.4. Smoke Emission

The variation in smoke opacity over the engine speed is shown in Figure 16. Overall, the RPO32MCO68 blend exhibited lower smoke opacity as compared to the baseline diesel fuel. It was observed that the smoke opacity was highest at 2000 rpm and gradually decreased as the engine speed increased. At 2000 rpm, the RPO32MCO68 biofuel blend showed similar smoke opacity to the diesel

fuel. However, the smoke opacity reduced by 10.4%, 29.4%, and 64.5% at 2500, 3000, and 3500 rpm, respectively. Lower smoke opacity was possibly due to the presence of oxygen content in the blend that allowed a more homogenous mixture for better combustion efficiency. Another possible explanation for this is that blended fuel contained less sulfur, which is believed to help reduce smoke opacity [44]. Meanwhile, diesel fuels containing aromatic hydrocarbon have a greater tendency to produce more smoke (soot) [45].

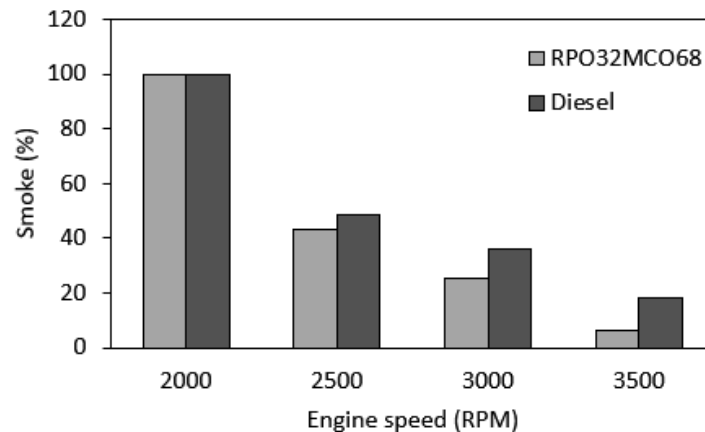


Figure 16. Comparison of smoke opacity as a function of engine speeds.

4. Conclusions

In this work, Melaleuca Cajuputi oil (MCO) was introduced as a new potential biofuel to be blended with refined palm oil (RPO) to formulate a new hybrid biofuel. The present study was performed in three phases. For the first phase, physicochemical properties of the hybrid biofuel blend were analyzed. Secondly, the key properties were optimized in accordance to the ASTM D6751/EN 14214 standards. Finally, the optimized blend was further examined to study its performance, combustion, and emission characteristics in a single cylinder diesel engine. From the results of this work, the following conclusions can be drawn:

1. It was found that MCO is mainly composed of 64.8% hydrocarbons (HC) and 34.6% oxygenated products. Higher percentage of HC contribute to high calorific value (CV) of MCO which indicated it as a potential source of biofuel. The presence of oxygenated products promote better combustion efficiency and lower smoke opacity.
2. The blend of high viscosity RPO with low viscosity MCO successfully reduced the viscosity and density of hybrid biofuel. The higher the fraction of MCO, the lower the viscosity and density of the blends. CV was increased with the increase of MCO in the blends.
3. The key properties of optimum hybrid biofuel (RPO32MCO68) obtained viscosity, density, and CV of 5.45 mm²/s, 880.20 kg/m³, and 42.1 MJ/kg respectively. These key properties were in accordance with the ASTM 6751/EN 14214 standards and demonstrated comparable properties to those of baseline diesel fuel.
4. At the entire range of speeds, in-cylinder peak pressure, brake torque, and brake power for the optimum hybrid biofuel blend were slightly lower than those of baseline diesel fuel. The largest drop in peak pressure, brake torque, and brake power are 10.7%, 21.4%, and 20.6%, respectively.
5. Notably, NO_x emission and smoke opacity were decreased as compared to diesel fuel across the speed range. The largest NO_x reduction was 17.3% and the smoke opacity reduction was 64.5% at maximum engine speed. Meanwhile, CO emission was found similar in comparison to diesel fuel. BSFC and HC emissions were found to be slightly higher than those of baseline diesel fuel.

- Overall, this study has shown that the RPO32MCO68 hybrid biofuel blend has successfully run a diesel engine with comparable engine performance and exhaust emissions to those of diesel fuel. This suggested that the blend is marked as a potential new source of biofuel.

Author Contributions: Conceptualization, S.C.M. and M.Y.I.; Methodology, S.C.M., M.Y.I. and Y.H.T.; Experimentation, S.C.M., M.F.H. and Y.H.T.; Data analysis, S.C.M., Y.H.T. and M.F.H.; Resources, M.Y.I. and M.F.H.; Writing—original draft preparation, S.C.M.; Writing—review and editing, Y.H.T., M.Y.I. and S.C.M.

Funding: This research was funded by the Ministry of Higher Education Malaysia and Universiti Sains Malaysia under the fundamental research grant (FRGS) scheme (FRGS/1/2016/TK07/USM/02/2; 203.PMEKANIK.6071356) and BRIDGING research grant scheme (304/PMEKANIK/6316119).

Acknowledgments: The authors would like to thank the engine laboratory staff who have provided technical support throughout the experimental work.

Conflicts of Interest: The authors declare no conflict of interest.

References

- Barnwal, B.K.; Sharma, M.P. Prospects of biodiesel production from vegetable oils in India. *Renew. Sustain. Energy Rev.* **2005**, *9*, 363–378. [[CrossRef](#)]
- Ashraful, A.M.; Masjuki, H.H.; Kalam, M.A.; Rizwanul Fattah, I.M.; Imtenan, S.; Shahir, S.A.; Mobarak, H.M. Production and comparison of fuel properties, engine performance, and emission characteristics of biodiesel from various non-edible vegetable oils: A review. *Energy Convers. Manag.* **2014**, *80*, 202–228. [[CrossRef](#)]
- Hellier, P.; Ladommatos, N.; Yusaf, T. The influence of straight vegetable oil fatty acid composition on compression ignition combustion and emissions. *Fuel* **2015**, *143*, 131–143. [[CrossRef](#)]
- Ndayishimiye, P.; Tazerout, M. Use of palm oil-based biofuel in the internal combustion engines: Performance and emissions characteristics. *Energy* **2011**, *36*, 1790–1796. [[CrossRef](#)]
- Emberger, P.; Hebecker, D.; Pickel, P.; Remmele, E.; Thuncke, K. Emission behaviour of vegetable oil fuel compatible tractors fuelled with different pure vegetable oils. *Fuel* **2016**, *167*, 257–270. [[CrossRef](#)]
- Li, Q.; Backes, F.; Wachtmeister, G. Application of canola oil operation in a diesel engine with common rail system. *Fuel* **2015**, *159*, 141–149. [[CrossRef](#)]
- Yusop, A.F.; Mamat, R.; Yusaf, T.; Najafi, G.; Yasin, M.H.M.; Khathri, A.M. Analysis of particulate matter (pm) emissions in diesel engines using palm oil biodiesel blended with diesel fuel. *Energies* **2018**, *11*, 1039. [[CrossRef](#)]
- Ramadhas, A.S.; Jayaraj, S.; Muraleedharan, C. Characterization and effect of using rubber seed oil as fuel in the compression ignition engines. *Renew. Energy* **2005**, *30*, 795–803. [[CrossRef](#)]
- Sidibé, S.S.; Blin, J.; Vaitilingom, G.; Azoumah, Y. Use of crude filtered vegetable oil as a fuel in diesel engines state of the art: Literature review. *Renew. Sustain. Energy Rev.* **2010**, *14*, 2748–2759. [[CrossRef](#)]
- Deepanraj, B.; Srinivas, M.; Arun, N.; Sankaranarayanan, G.; Abdul Salam, P. Comparison of jatropha and karanja biofuels on their combustion characteristics. *Int. J. Green Energy* **2017**, *14*, 1231–1237. [[CrossRef](#)]
- Chauhan, B.S.; Singh, R.K.; Cho, H.M.; Lim, H.C. Practice of diesel fuel blends using alternative fuels: A review. *Renew. Sustain. Energy Rev.* **2016**, *59*, 1358–1368. [[CrossRef](#)]
- Santhosh, M.; Padmanaban, K.P. Experimental investigation on engine performances, combustion characteristics and emission of exhaust gases of VCR engine fuelled with cottonseed oil methyl ester blended with diesel. *Int. J. Green Energy* **2014**, *13*, 1534–1545. [[CrossRef](#)]
- Adam, I.; Abdul Aziz, A.; Heikal, M.; Yusup, S.; Firmansyah; Ahmad, A.; Zainal Abidin, E. Performance and emission analysis of rubber seed, palm, and their combined blend in a multi-cylinder diesel engine. *Energies* **2018**, *11*, 1522. [[CrossRef](#)]
- Rahman, M.; Rasul, M.; Hassan, N.; Hyde, J. Prospects of biodiesel production from macadamia oil as an alternative fuel for diesel engines. *Energies* **2016**, *9*, 403. [[CrossRef](#)]
- Rahman, M.; Rasul, M.; Hassan, N. Study on the tribological characteristics of Australian native first generation and second generation biodiesel fuel. *Energies* **2017**, *10*, 55. [[CrossRef](#)]
- Gui, M.M.; Lee, K.T.; Bhatia, S. Feasibility of edible oil vs. non-edible oil vs. waste edible oil as biodiesel feedstock. *Energy* **2008**, *33*, 1646–1653. [[CrossRef](#)]

17. Rahman, S.M.A.; Nabi, M.N.; Van, T.C.; Suara, K.; Jafari, M.; Dowell, A.; Islam, M.A.; Marchese, A.J.; Tryner, J.; Hossain, M.F.; et al. Performance and Combustion Characteristics Analysis of Multi-Cylinder CI Engine Using Essential Oil Blends. *Energies* **2018**, *11*, 738. [[CrossRef](#)]
18. Kasiraman, G.; Nagalingam, B.; Balakrishnan, M. Performance, Emission and combustion improvements in a direct injection diesel engine using cashew nut shell oil as fuel with camphor oil blending. *Energy* **2012**, *47*, 116–124. [[CrossRef](#)]
19. Vallinayagam, R.; Vedharaj, S.; Yang, W.M.; Raghavan, V.; Saravanan, C.G.; Lee, P.S.; Chua, K.J.E.; Chou, S.K. Investigation of evaporation and engine characteristics of pine oil biofuel fumigated in the inlet manifold of a diesel engine. *Appl. Energy* **2014**, *115*, 514–524. [[CrossRef](#)]
20. Hoki, M.; Takeda, S.; Ito, N.; Yazawa, H. *Engine Performance by Eucalyptus Oil Blended Fuel*; Bulletin of the Faculty of Agriculture; Mie University: Mie, Japan, December 1981.
21. Poola, R.B.; Nagalingam, B.; Gopalakrishnan, K.V. Performance studies with biomass-derived high-octane fuel additives in a two-stroke spark-ignition engine. *Biomass Bioenergy* **1994**, *6*, 369–379. [[CrossRef](#)]
22. Devan, P.K.; Mahalakshmi, N.V. A study of the performance, emission and combustion characteristics of a compression ignition engine using methyl ester of paradise oil–eucalyptus oil blends. *Appl. Energy* **2009**, *86*, 675–680. [[CrossRef](#)]
23. Vallinayagam, R.; Vedharaj, S.; Yang, W.M.; Lee, P.S.; Chua, K.J.E.; Chou, S.K. Pine oil–biodiesel blends: A double biofuel strategy to completely eliminate the use of diesel in a diesel engine. *Appl. Energy* **2014**, *130*, 466–473. [[CrossRef](#)]
24. Kommana, S.; Banoth, B.N.; Kadavakollu, K.R. Performance and emission of VCR-CI engine with palm kernel and eucalyptus blends. *Perspect. Sci.* **2016**, *8*, 195–197. [[CrossRef](#)]
25. Sakasegawa, M.; Hori, K.; Yatagai, M. Composition and antitermite activities of essential oils from melaleuca species. *J. Wood Sci.* **2003**, *49*, 181–187. [[CrossRef](#)]
26. Southwell, I.; Lowe, R. *Tea Tree: The Genus Melaleuca*; Harwood Academic Publishers: Amsterdam, The Netherlands, 1999.
27. Schimleck, L.R.; Doran, J.C.; Rimbawanto, A. Near infrared spectroscopy for cost effective screening of foliar oil characteristics in a melaleuca cajuputi breeding population. *J. Agric. Food Chem.* **2003**, *51*, 2433–2437. [[CrossRef](#)] [[PubMed](#)]
28. Oyen, L.P.A.; Dung, N.X. *Plant Resources of South East Asia 19: Essential-Oil Plants*; Backhuys Publishers: Leiden, The Netherlands, 1999.
29. Jajaei, S.M.; Daud, W.R.W.; Markom, M.; Zakaria, Z.; Presti, M.L.; Costa, R.; Mondello, L.; Santi, L. Extraction of Melaleuca cajuputi using supercritical fluid extraction and solvent extraction. *J. Essent. Oil Res.* **2010**, *22*, 205–210. [[CrossRef](#)]
30. Silva, C.J.; Barbosa, L.C.A.; Maltha, C.R.A.; Pinheiro, A.L.; Ismail, F.M.D. Comparative study of the essential oils of seven Melaleuca (Myrtaceae) species grown in Brazil. *Flavour Fragr. J.* **2007**, *22*, 474–478. [[CrossRef](#)]
31. Mat Yasin, M.H.; Mamat, R.; Najafi, G.; Ali, O.M.; Yusop, A.F. Potentials of palm oil as new feedstock oil for a global alternative fuel: A review. *Renew. Sustain. Energy Rev.* **2017**, *79*, 1034–1049. [[CrossRef](#)]
32. Ong, H.C.; Mahlia, T.M.I.; Masjuki, H.H.; Honnery, D. Life cycle cost and sensitivity analysis of palm biodiesel production. *Fuel* **2012**, *98*, 131–139. [[CrossRef](#)]
33. Reham, S.S.; Masjuki, H.H.; Kalam, M.A.; Shancita, I.; Rizwanul Fattah, I.M.; Ruhul, A.M. Study on stability, fuel properties, engine combustion, performance and emission characteristics of biofuel emulsion. *Renew. Sustain. Energy Rev.* **2015**, *52*, 1566–1579. [[CrossRef](#)]
34. Giuliano Albo, P.A.; Lago, S.; Wolf, H.; Pagel, R.; Glen, N.; Clerck, M.; Ballereau, P. Density, viscosity and specific heat capacity of diesel blends with rapeseed and soybean oil methyl ester. *Biomass Bioenergy* **2017**, *96*, 87–95. [[CrossRef](#)]
35. Melo-Espinosa, E.A.; Piloto-Rodríguez, R.; Goyos-Pérez, L.; Sierens, R.; Verhelst, S. Emulsification of animal fats and vegetable oils for their use as a diesel engine fuel: An overview. *Renew. Sustain. Energy Rev.* **2015**, *47*, 623–633. [[CrossRef](#)]
36. NguyenThi, T.; Bazile, J.-P.; Bessières, D. Density measurements of waste cooking oil biodiesel and diesel blends over extended pressure and temperature ranges. *Energies* **2018**, *11*, 1212. [[CrossRef](#)]
37. Motl, O.; Hodačová, J.; Ubik, K. Composition of Vietnamese cajuput essential oil. *Flavour Fragr. J.* **1990**, *5*, 39–42. [[CrossRef](#)]

38. Torri, I.D.V.; Paasikallio, V.; Faccini, C.S.; Huff, R.; Caramão, E.B.; Sacon, V.; Oasmaa, A.; Zini, C.A. Bio-oil production of softwood and hardwood forest industry residues through fast and intermediate pyrolysis and its chromatographic characterization. *Bioresour. Technol.* **2016**, *200*, 680–690. [[CrossRef](#)] [[PubMed](#)]
39. Kommana, S.; Naik Banoth, B.; Radha Kadavakollu, K. Eucalyptus-palm kernel oil blends: A complete elimination of diesel in a 4-stroke vcr diesel engine. *J. Combust.* **2015**, *2015*, 182879. [[CrossRef](#)]
40. Pinzi, S.; Garcia, I.L.; Lopez-Gimenez, F.J.; Luque de Castro, M.D.; Dorado, G.; Dorado, M.P. The ideal vegetable oil-based biodiesel composition: A review of social, economical and technical implications. *Energy Fuels* **2009**, *23*, 2325–2341. [[CrossRef](#)]
41. Laza, T.; Bereczky, Á. Basic fuel properties of rapeseed oil-higher alcohols blends. *Fuel* **2011**, *90*, 803–810. [[CrossRef](#)]
42. Meher, L.C.; Vidya Sagar, D.; Naik, S.N. Technical aspects of biodiesel production by transesterification—A review. *Renew. Sustain. Energy Rev.* **2006**, *10*, 248–268. [[CrossRef](#)]
43. Wang, Y.D.; Al-Shemmeri, T.; Eames, P.; McMullan, J.; Hewitt, N.; Huang, Y.; Rezvani, S. An experimental investigation of the performance and gaseous exhaust emissions of a diesel engine using blends of a vegetable oil. *Appl. Therm. Eng.* **2006**, *26*, 1684–1691. [[CrossRef](#)]
44. Rakopoulos, D.C.; Rakopoulos, C.D.; Giakoumis, E.G.; Dimaratos, A.M.; Founti, M.A. Comparative environmental behavior of bus engine operating on blends of diesel fuel with four straight vegetable oils of Greek origin: Sunflower, cottonseed, corn and olive. *Fuel* **2011**, *90*, 3439–3446. [[CrossRef](#)]
45. Mohan, B.; Yang, W.; Raman, V.; Sivasankaralingam, V.; Chou, S.K. Optimization of biodiesel fueled engine to meet emission standards through varying nozzle opening pressure and static injection timing. *Appl. Energy* **2014**, *130*, 450–457. [[CrossRef](#)]



© 2018 by the authors. Licensee MDPI, Basel, Switzerland. This article is an open access article distributed under the terms and conditions of the Creative Commons Attribution (CC BY) license (<http://creativecommons.org/licenses/by/4.0/>).